



## The benefit of using access materials for soil stress reduction depends on the material's properties and vehicle mean ground pressure<sup>☆</sup>



Loraine ten Damme <sup>a,b,\*</sup> , Matthias Stettler <sup>c</sup> , Renato P. de Lima <sup>d</sup> , Thomas Keller <sup>a,e</sup>

<sup>a</sup> Swedish University of Agricultural Sciences (SLU), Department of Soil and Environment, Box 7014, SE-75007 Uppsala, Sweden

<sup>b</sup> Aarhus University, Department of Agroecology, Research Centre Viborg, Blichers Allé 20, P.O. Box 50, DK-8830 Tjele, Denmark

<sup>c</sup> Beratungsbüro Matthias Stettler, 3251 Wengi b. Büren, Switzerland

<sup>d</sup> Agricultural Engineering College (FEAGRI), University of Campinas (UNICAMP), Av. Cândido Rondon, 501 – Cidade Universitária, Campinas – SP, 13083-875, Brazil

<sup>e</sup> Agroscope, Department of Agroecology and Environment, Reckenholzstrasse 191, CH-8046 Zürich, Switzerland

### ARTICLE INFO

#### Keywords:

Balling probes

Construction machines

Finite element modelling

Infrastructure construction

Mean normal stress

Soil compaction

Soil protection material

Temporary matting

### ABSTRACT

Construction activities can induce soil compaction due to the use of heavy vehicles and repeated vehicle passes. Driving on access material reduces the risk of compaction, but data on soil stress reduction are lacking. This study investigated the effect of three access materials (0.5 m thick sand track, 0.3 m thick timber mattresses, and 0.1 m thick composite mats) on soil stress, relative to driving on unprotected soil. Mean normal stress was measured at 0.2 and 0.4 m soil depths for tracked and tyred construction vehicles (bulldozer, excavator, dump truck, and tractor-trailer). We used finite element modelling to investigate the effect of material's thickness and stiffness on soil stress reduction. Measurements revealed that driving on access material reduced soil stress by 21–77 % and 0–60 % at 0.2 and 0.4 m depths, respectively. Stress reduction increased with increasing mean ground pressure and was larger for tyred than for tracked vehicles. The tested access materials reached a comparable effect, but simulations indicated that additional stress reduction could be achieved by increasing the stiffness or thickness of the material. Thus, more rigid or thicker material achieve greater soil stress reductions. These characteristics should be balanced against costs, transport, and ease of handling of the material.

### 1. Introduction

Soils contribute to a comfortable life on Earth by providing food, feed and fibre, storing more carbon than the amount that resides in the atmosphere and plants together, and being the most biodiverse singular habitat on Earth, among other functions (e.g., Anthony et al., 2023; Janzen, 2005). The extent to which a soil can perform functions is sensitive to soil threats such as soil sealing, soil pollution, and soil compaction (Stolte et al., 2015). Estimates of already degraded and degrading soils amount to 60 % and to 33 % of soils in Europe and worldwide, respectively (European Commission: Joint Research Centre et al., 2024; FAO and ITPS, 2015). Hence, protecting soils against degradation is vital.

Considering infrastructure construction activities, such as the expansion and linking of energy supply systems or below- and above-ground transportation systems, the risk of soil compaction is evident. Construction activities typically involve heavy vehicles and equipment,

including weights up to 800 kN (Horn et al., 2021) for transport or hauling of materials. Excavators or a dumper with a container can weigh 400 kN (The European Parliament and the Council, 2015). Such loads may exceed soil bearing capacity. Vehicle traffic on construction sites is often concentrated in traffic lanes and temporary roads that are particularly at risk of soil compaction as soil is frequently stressed by repeated wheeling. The risk of soil compaction is especially great when activities take place under moist soil conditions, when soil strength is low (Berli et al., 2003; Thompson et al., 2022).

Few studies exist on the effects of construction traffic on soil compaction (but see Berli et al., 2003; Horn et al., 2021; Najafi et al., 2019; Thompson et al., 2022). Berli et al. (2003) reported that a dry loess soil in Switzerland could resist deformation during three passes of a vehicle equipped with steel tracks (weight 251–372 kN, mean ground pressure 42–78 kPa), whilst the rewetted soil was too weak to resist compaction. Horn et al. (2021) investigated soil physical and hydrological characteristics in traffic lanes used for gas pipeline hauling in

<sup>☆</sup> This article is part of a special issue entitled: 'Soil behavior and traffic' published in Journal of Terramechanics.

\* Corresponding author at: Swedish University of Agricultural Sciences (SLU), Department of Soil and Environment, Box 7014, SE-75007 Uppsala, Sweden.

E-mail address: [ltd@agro.au.dk](mailto:ltd@agro.au.dk) (L. ten Damme).

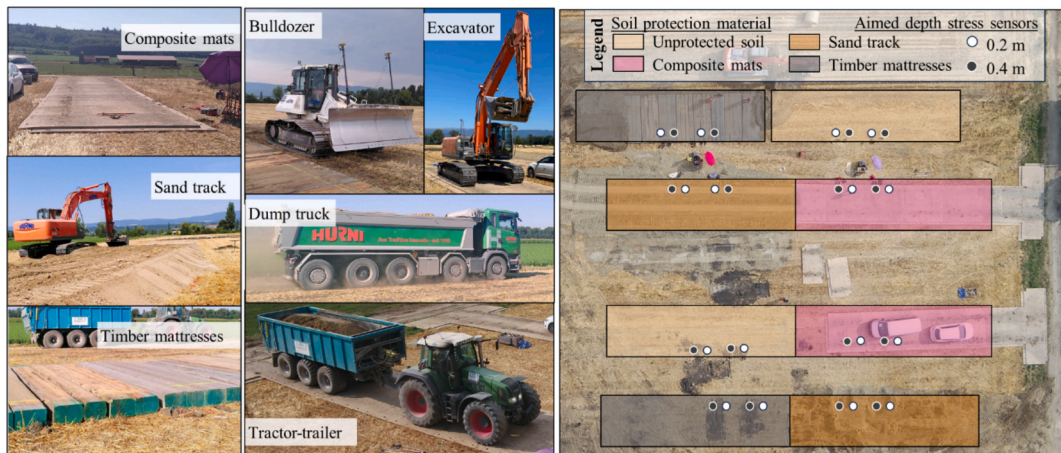


**Fig. 1.** Experimental set-up (from left to right: tested access materials; used vehicles; experimental layout). See Table 1 for characteristics of the access materials and Table 3 for the loading characteristics of the vehicles.

Northern Germany immediately after closure of the pipeline trenches and after three years. The authors verified harmful soil degradation to 0.8 m soil depth in the traffic lanes, including a 10 % increase in dry bulk density and reduced saturated hydraulic conductivity as compared to adjacent arable soil, with no improvements after three years. Thompson et al. (2022) measured higher dry bulk density and penetration resistance in the surface soil layer as well as reduced surface infiltration rates following construction traffic on sandy and loamy prairie grassland in southeast Alberta, Canada. They also observed that the use of timber mattresses as access material – a material installed, overlying the existing soil – reduced the impact of traffic. Similarly, Najafi et al. (2019) found that the use of access material on mixed grass Prairie soils (southeast Alberta) limited the impact of construction traffic on soil and vegetation.

Driving on access material protects soil structure by distributing a vehicle's load over a larger area (Gartrell et al., 2009; Najafi et al., 2019; Solgi et al., 2018), which lowers the mean ground pressure and hence exerts lower mechanical stresses into the soil. This also implies that the reduction of soil stress by using access material might differ between vehicles with tyres and tracks, as tracks have a larger contact area and therefore often a lower mean ground pressure than tyres. In practice, access materials are primarily used to enhance work efficacy, particularly on soft soils. The reduction of wheel slip by preventing direct interaction between wheel and soil optimises tractive efficiency and thereby decreases fuel use (Ashok Kumar et al., 2017; Jenane et al., 1996). Moreover, topsoil deformation can increase soil pore water pressure, and cause water-saturated conditions and smearing of soil (Horn et al., 1994), which further increases slip and may result in safety-issues and delays of construction work.

Different access materials are available, such as timber mats, composite mats, steel mats, sand beds, as well as tree and shrub branches and sawdust but these are mainly used in forestry. So far, direct comparison of the effect of different access materials on soil compaction are limited. Solgi et al. (2018) made an assessment of rut formation and soil dry bulk

density after driving with a 10-Mg tyred skidder on branches, sawdust and a combination of branches and sawdust of different densities (0, 10 and 20 kg m<sup>-2</sup>) in a mountainous forest. They concluded that 'heavier mats' were more effective in reducing adverse effects than 'lighter mats' as long as the mat layers remained intact, and that mats of branches outperformed sawdust and sawdust-branch mats. Their findings shows that differences in the extent to which access materials protect soil against compaction depends on material properties.

We found no published literature on the effect of different types of access materials on the propagation of mechanical stress into the soil. Moreover, no study so far has investigated if the protective effect of access material differs between vehicle characteristics, e.g., between tyred and tracked undercarriage systems. Data and improved understanding of soil stress reduction by different access materials could encourage the use of access materials for soil protection on construction sites and in other situations, provide guidance for the choice of access material, and optimize the design of such access materials. With these knowledge gaps in mind, we conducted in-situ soil stress measurements in a field experiment and carried out complementary numerical simulations. The main aim of this study was to enhance the understanding of the effect of access materials on soil stress during traffic by tracked and tyred vehicles. The hypotheses of this study were that i) access material reduces soil stress; ii) access materials reduce stress less below tracks compared to tyres, and iii) stiffness and thickness of the access material influences the stress reduction.

## 2. Material and methods

A field experiment was carried out to measure soil mean normal stress at two soil depths during wheeling on unprotected soil surface and on three types of access materials with typical transportation and construction vehicles with tracked and tyred undercarriage systems (Fig. 1). Soil samples were taken from reference soil (non-trafficked soil) for textural, structural, and mechanical soil characterisation. Finite element

**Table 1**

Characteristics of the tested access materials.

Access material	Length <sup>[1]</sup> , m	Width, m	Height, m	Mass <sup>[1]</sup> , kg	Density, kg m <sup>-3</sup>	Mass per running metre, kg m <sup>-1</sup>
Composite mats <sup>[2]</sup>	2.44	4.27	0.12	450	407	184
Timber mattresses	1.20–1.60	5.00	0.30	750–1000 <sup>[3]</sup>	415 <sup>[4]</sup>	625
Sand track	nd	4.00	0.4–0.5	nd	1520–1680 <sup>[5]</sup>	2432–3360

nd = not defined. <sup>[1]</sup> per modular segment (composite mats) and per timber mattress including three to four logs, each having a longitudinal dimension (length) of approximately 0.4 m. <sup>[2]</sup> based on Newpark Resources, Inc., (n.d.) <sup>[3]</sup> calculated from the volume and density, <sup>[4]</sup> average dried weight for spruce. <sup>[5]</sup> estimated (e.g., civiltoday, n.d.).

**Table 2**

Soil characteristics of the experimental site.

Soil depth, m	Clay <sup>[1]</sup> , %	Silt <sup>[1]</sup> , %	Sand <sup>[1]</sup> , %	SOC, %	$\rho_p$ , Mg m <sup>-3</sup>	$\rho_b$ , Mg m <sup>-3</sup>	$\Theta_v$ , m <sup>3</sup> m <sup>-3</sup>	$\phi$ , m <sup>3</sup> m <sup>-3</sup>	$S$ , %
0–0.2	43.3	51.3	5.5	7.2	2.47	0.92	0.52	0.62	82.6
0.2–0.4	50.8	43.4	5.8	6.3	2.61	1.15	0.51	0.57	89.9

<sup>[1]</sup> Clay <2 µm, silt 2–50 µm, sand >50 µm. SOC = Soil organic carbon,  $\rho_p$  = particle density,  $\rho_b$  = dry bulk density,  $\Theta_v$  = volumetric soil water content,  $\phi$  = soil pore volume,  $S$  = degree of saturation ( $S = 100 * \Theta_v / \phi$ ).

**Table 3**

Loading characteristics of the vehicles.

Machine	Axle	Category	Dimensions	$F$ <sup>[1]</sup> , Mg	$A$ <sup>[2]</sup> , m <sup>2</sup>	$p_{tyre}$ <sup>[3]</sup> , kPa	$p_{mean}$ <sup>[4]</sup> , kPa
Bulldozer	—	Track	3.20×0.86 <sup>[5]</sup>	8.0	2.72	—	29
Excavator	—	Track	3.90×0.60 <sup>[5]</sup>	10.5	2.31	—	45
Tractor	Front	Tyre	540/65 R34	1.6	0.21	165	75
Tractor	Rear	Tyre	650/75 R38	4.2	0.38	190	107
Trailer	Front	Tyre	650/50 R22.5	4.7	0.28	365	165
Trailer	Middle	Tyre	650/50 R22.5	5.0	0.27	395	182
Trailer	Rear	Tyre	650/50 R22.5	5.0	0.27	375	182
Dump truck	Front	Tyre	385/65 22.5	3.5	0.15	700	223
Dump truck	Second	Tyre	385/65 22.5	3.3	0.15	700	207
Dump truck	Third	Tyre <sup>[6]</sup>	315/80 R22.5	4.7	0.13 <sup>[7]</sup>	700	183 <sup>[7]</sup>
Dump truck	Fourth	Tyre <sup>[6]</sup>	315/80 R22.5	5.3	0.13 <sup>[7]</sup>	700	206 <sup>[7]</sup>
Dump truck	Rear	Tyre	385/65 22.5	3.8	0.15	700	242

<sup>[1]</sup>  $F$  = static track or wheel load; <sup>[2]</sup>  $A$  = ground contact area per single track or single tyre, for the tracks calculated from their dimensions, for the tractor-trailer tyres estimated with help of [www.Terranimo.world](http://www.Terranimo.world), and for the dump truck approximated from field measurements; <sup>[3]</sup>  $p_{tyre}$  = tyre inflation pressure; <sup>[4]</sup>  $p_{mean}$  = mean ground pressure calculated from  $F$  and  $A$ . <sup>[5]</sup> = length x width (m) of ground contact for a single track; <sup>[6]</sup> dual tyre. <sup>[7]</sup> = per single tyre. Note that the tractor front axle is not presented in the results.

modelling was employed to investigate the effect of the access material thickness and stiffness on stress reduction.

## 2.1. Field experiment

### 2.1.1. Experimental factors

Soil mean normal stress was measured under three types of access material and beneath the unprotected soil surface. The soil was a silty clay with high soil organic carbon content (Table 2). Dry bulk density was 0.92 and 1.15 Mg m<sup>-3</sup> and the volumetric soil water content at the time of experimental traffic was 0.52 and 0.51 m<sup>3</sup> m<sup>-3</sup> at 0.2 and 0.4 m depth, respectively (Table 2). The three types of access materials were: composite mats (DURA-BASE® Advanced-Composite Mats ([Newpark Resources, Inc.](http://NewparkResources.com), The Woodlands, TX, USA), with modular segments that can be clicked into one another), timber mattresses (existing of three or four logs joined by a steel strapping), and sand tracks containing a mix of sand and gravel (Fig. 1, Table 1). The sand tracks were distributed by an excavator and compacted by a 16-Mg bulldozer.

Experimental traffic was performed by two vehicles with a metal-track undercarriage system – a 16-Mg bulldozer and 21-Mg excavator – and by two vehicles equipped with tyres – a tractor-trailer combination

with four axles, 40.9 Mg in total, and a five-axle 41.1-Mg dump truck (Fig. 1). The loading characteristics are presented in Table 3.

### 2.1.2. Experimental layout

The field experiment was executed in two blocks with four treatments (i.e., three access materials and an unprotected soil surface) were distributed over the two driveways (Fig. 1). The experiment took place on an arable site near Kallnach, Switzerland (47°00'52.8"N 7°12'46.4"E), in July 2022 after harvest of spring barley (*Hordeum vulgare*) and was conducted at soil conditions slightly drier than field capacity, i.e., at a matric potential slightly more negative than -100 hPa (at which the volumetric soil water content equalled 0.54 m<sup>3</sup> m<sup>-3</sup>). In each treatment per block, stress sensors were installed (Section 2.1.3) for quantification of soil mean normal stress during traffic. Vehicle speed ranged from 3 to 5 km hr<sup>-1</sup> to ensure good soil stress readings. Vehicles always passed in the order: bulldozer, excavator, tractor-trailer, and dump truck, i.e., with increasing mean ground pressure (Table 3).

### 2.1.3. Soil stress measurements

Bolling probes (Bolling, 1987) were used for quantification of soil mean normal stress ( $\sigma_m$ ) during traffic at aimed soil depths of 0.2 and at

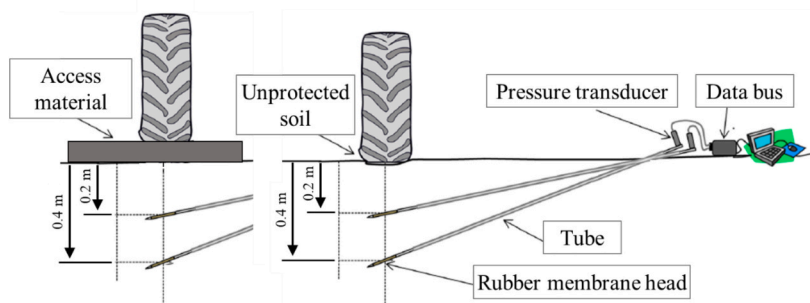


**Fig. 2.** Schematic illustration of the set-up for soil stress measurements, with Bolling probes placed at two different soil depths (adapted from Keller et al. (2016)). See Supplementary Fig. S1 for typical stress-curve measured under track and tyre.

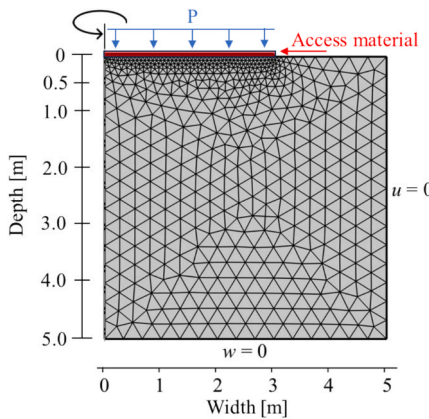


**Fig. 3.** Mesh, applied surface pressure  $P$  (acting on the access material), and boundary conditions of the finite element model, where  $u$  is the displacement in the radial (horizontal) direction and  $w$  is the displacement in the axial (vertical) direction of the soil domain. The problem was modelled for an axisymmetric situation (5 m in depth and 10 m width).

0.4 m (Fig. 2). The probes consist of a rubber membrane head (inner diameter 10 mm, length 150 mm) at the end of a tube with similar diameter as the membrane head. These probes were filled with an incompressible fluid (water) and connected to a syringe, with which an initial pressure of about 100 kPa was applied to secure good sensor-soil contact. Closing off the valve led the inclusion pressure ( $p_i$ ) to be measured in a pressure transducer. The transducers were connected to a data bus, and pressures were recorded every 0.04 s. The inclusion pressures were converted to mean normal stress following the approach outlined by Berli et al. (2006, eqs. 20 and 23):  $\sigma_m = p_i / (3(1-\nu)/(1+\nu))$ , where  $\nu$  is the Poisson's ratio that was estimated from uniaxial compression tests (Section 2.1.4).

Two probes were installed per depth, treatment and block, and inserted into holes drilled at predefined angles guided by a metal frame. The use of this frame allowed the lateral position of the membrane heads to be marked and provided for the vehicle drivers to steer the machines so that the centreline of the tracks and tyres passed over the sensors (Fig. 2). The position of the membrane head relative to the centreline of the wheel rut was confirmed after all 16 passes were completed when the probes were carefully dug free. The depth of the membrane head relative to the undisturbed soil surface was also assessed.

#### 2.1.4. Soil mechanical characterisation

Soil cores (471 cm<sup>3</sup>; 6 cm high, 10 cm diameter) sampled at 0.2 and 0.4 m depths in undisturbed areas in between the plots were used for obtaining the Young's modulus,  $E$ , and the Poisson's ratio,  $\nu$ . These properties were determined from stress-strain curves from uniaxial compression tests performed with a 08.67 Compression test apparatus set (Royal Eijkelkamp, Giesbeek, The Netherlands).

The Young's modulus was derived from stress-strain curves of unconfined compression tests, i.e., on soil samples taken out of their cylindrical ring. Each sample was stepwise loaded from 0 to 30 kPa with a 5-kPa increment, then unloaded, and reloaded stepwise up to 50 kPa. Each load was maintained for one minute. The Young's modulus of each soil core was defined as the slope of the linear part of the reloading curve. The Young's modulus of the soil prior to wheeling was then calculated as the geometric mean of all soil cores sampled at a given depth.

The Poisson's ratio was defined using Eq. (1) following Eggers et. al (2006), i.e., based on the reloading curve of confined compression tests (i.e., soil samples contained in their cylindrical ring) and the Young's modulus:

$$\nu = \frac{1}{4} \left[ \frac{\varepsilon_z E}{\sigma_z} + \left\{ \left( 1 - \frac{\varepsilon_z}{\sigma_z} E \right) \right\}^{0.5} - 1 \right] \quad (1)$$

In the confined compression tests, samples were stepwise loaded to 10, 15, 30 and 50 kPa, unloaded, and reloaded to 5, 10, 15, 30, 50, 75, 100, 200, 400 and 800 kPa. Each load was maintained for one minute. The Poisson's ratio of each soil core was defined as the slope of the linear part of the reloading curve up to 75 kPa. The Poisson's ratio of the soil prior to wheeling was then calculated as the geometric mean of all soil cores sampled at a given depth. We obtained Young's modulus values of 2090 and 3936 kPa for the 0.2 and 0.4 m depths, respectively. Poisson's ratios were 0.33 and 0.43 for the 0.2 and 0.4 m depths, respectively.

#### 2.2. Finite element modelling

Numerical simulations were carried out using the finite element method (FEM) within the framework of COMSOL Multiphysics Version 6.3 (COMSOL Inc., Stockholm, Sweden). The model was formulated as an axisymmetric problem (5 m radius, 5 m depth). The displacements in the radial (horizontal) direction,  $u$ , and the displacement in the axial (vertical) direction at the lower boundary,  $w$ , were restricted (i.e., equal to 0) (Fig. 3). A plate with variable thickness (0.05 to 0.8 m) and a diameter of 6 m was positioned on the surface of the soil domain to simulate an access material. A free triangular mesh with approximately 1029 elements (slightly varying for different simulation scenarios) was applied to the model.

Simulation scenarios consisted of varying the thickness and Young's modulus of the access material. We used a linear elastic model for the soil domain and access material. Young's modulus of the soil was 3000 kPa (a typical value for cohesive soil) in all simulations. Poisson's ratio of soil and access material was 0.33. Simulations were carried out by varying the Young's modulus of the access material between  $3 \times 10^3$  kPa (i.e., as soil) and  $3 \times 10^8$  kPa, to represent a range of soft to hard materials. The access material's thickness was set to 0.05, 0.1, 0.4 or 0.8 m for the different simulations. For each simulation, we applied a surface load of 200 kPa and took the mean normal stress under the centreline of the load axis at 0.2 and 0.4 m depth for further considerations.

#### 2.3. Data handling and statistical analyses

Measurements under the tractor's front axle were excluded as this tyre did not pass the probes with its centreline due to the smaller track width of the tractor's front axle compared to its rear axle. Measurements with stress readings  $< 1$  kPa as well as one extreme outlier (251 kPa) were excluded. Readings from two probes aimed at 0.2 m depth could not be considered at 0.2 m depth as their effective depth was greater. Stress readings were minimally affected by repeated passes, which allowed us to calculate an average stress across the four vehicle passes for each axle, access material, and soil depth.

The relative soil mean normal stress ( $\sigma_{m-rel}$ ) was calculated to analyse the extent to which the access materials reduced soil stress and was calculated following Eq. (2), i.e., as the ratio of stress measured beneath the access material ( $\sigma_{m-AM}$ ) to soil stress beneath the unprotected soil surface ( $\sigma_{m-USS}$ ) for each depth ( $d$ ).

$$\sigma_{m-rel[d]} = \frac{\sigma_{m-AM[d]}}{\sigma_{m-USS[d]}} \quad (2)$$

A value of 1 indicates equal magnitude of stress when driving on access material as compared to driving on the unprotected soil surface, whilst the lower the ratio, the higher the relative stress reduction. The stress reduction factor is then expressed as  $1 - \sigma_{m-rel}$ .

Differences in absolute soil mean normal stress were analysed between treatments (i.e., access materials as well as unprotected soil), soil depths and undercarriage systems (i.e., tyres and tracks). The mean normal stress was fitted using the Linear Mixed-Effects Models of the

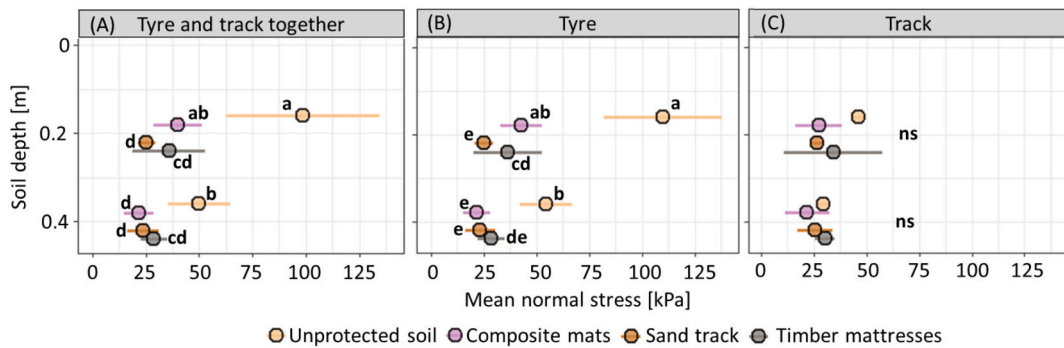


**Fig. 4.** Measured mean normal stress at 0.2 and 0.4 m soil depth (circle denotes mean and each half horizontal line one standard deviation), for both undercarriage systems (A) and split for tyres (B) and tracks (C). Different letters indicate significant differences at the 0.05 significance level within each subfigure, across soil depths.

lme4-package (Bates et al., 2015) version 1.1.35.5 in R (R Core team, 2024), with treatment, soil depth and undercarriage system as main effects. Block and driveway-within-block were added as random effects to account for potential spatial variation. Differences in soil mean normal stress were also analysed for tyres and tracks separately, following the model as described without undercarriage system as a factor. A contrast specification (sum to zero) for the main effects was provided using the 'contr.sum' function for acquiring the Type III sums of squares to account of interaction effects. The model-assumptions in terms of the distribution of the residuals and heteroscedasticity were checked visually and required a log10-transformation of both the soil mean normal stress and the relative soil mean normal stress. The Type III ANOVA was used to compute the analyses of variance tables, and the posthoc test emmeans from the R-package emmeans (Lenth, 2024) version 1.10.6 was used for the three two-way interactions of the main factors for which  $P < 0.05$ .

### 3. Results and discussion

#### 3.1. Access material reduces soil stress

Driving on the access materials significantly reduced soil stress at both soil depths (Fig. 4, Supplementary Fig. S2). The differences in stress at a given depth between the three access materials were minor

compared to the difference between access material and unprotected soil surface. For vehicles with tyres, soil mean normal stress was reduced by 61–77 % and by 47–60 % at 0.2 and 0.4 m depth, respectively, by driving on access material. For the tracked vehicles, soil stress was reduced by 21–42 % and by 0–26 % at 0.2 and 0.4 m depth, respectively, by driving on access material, yet these reductions did not result in significant differences. Mean normal stresses per axle, soil depth, and access material are presented in **Supplementary Fig. S3**.

The reduction in soil stress by driving on access materials supports this study's first hypothesis, whilst the difference in response between tyres and tracks is in support of the second hypothesis. The difference between the two types of undercarriage systems likely relates to differences in mean ground pressure. Driving with tyres on access material distributes a vehicle's mass over a larger area before being transferred to the soil, which significantly reduces soil stress (Gartrell et al., 2009; Najafi et al., 2019). Tracks utilise a larger contact area than tyres, i.e., distribute a vehicle's load over a large area also when driving directly on soil. The benefit of driving on access materials is therefore smaller for tracks. Nevertheless, soil stress under tracked vehicles was lower with access materials (although not significantly), and stress reduction is expected to be larger for tracked vehicles with a higher mean ground pressure. Moreover, driving tracked vehicles on access material protects soil structure by preventing direct interaction between track and soil, and hence limits distortion of the upper soil layers despite the lesser

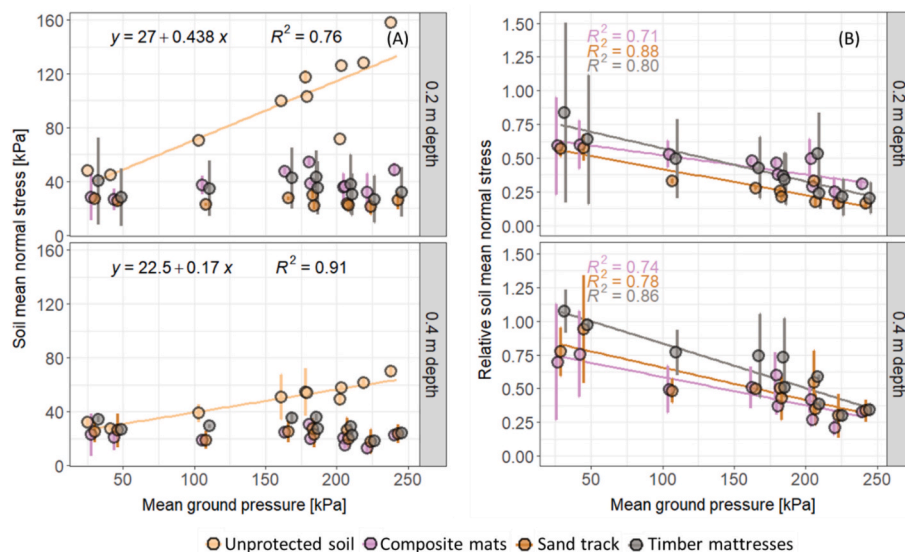


**Fig. 5.** A) Measured soil mean normal stress, and B) relative soil mean normal stress as a function of mean ground pressure, for 0.2 and 0.4 m soil depth (circle denotes mean and each half vertical line one standard deviation). Note that the data points are slightly offset on the x-axis to prevent complete overlap.

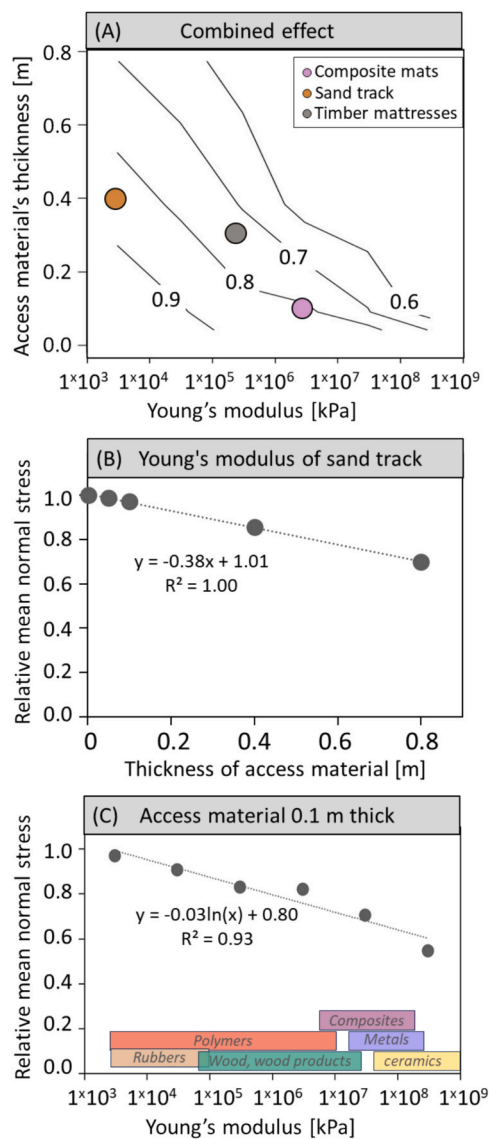


**Fig. 6.** Relative mean normal stress at 0.4 m soil depth when driving on access material (200 kPa surface load applied) as a function of the Young's modulus and thickness of the access material as numerically simulated. A relative stress of 1 equals the stress when driving on unprotected soil surface. **Fig. 6A** shows the combined effect, where the values inside the plot represent the relative soil mean normal stress for a given thickness (y-axis) and Young's modulus (x-axis). See **Supplementary Fig. S5** for effect on the relative mean normal stress at 0.2 m depth.

stress reduction than for tyres.

### 3.2. Stress reduction depends on mean ground pressure

Driving on access material reduced soil stress more strongly for tyres having high mean ground pressure than for tyres or tracks having low mean ground pressure. This is reflected in a decreasing relative mean normal stress with increasing mean ground pressure (Fig. 5). Mean normal stress was strongly positively correlated with mean ground pressure when driving on the unprotected soil surface, with exception of the dump truck's fourth axle (at  $p_{mean} = 206$  kPa) (Fig. 5A). In a study including 16 agricultural tyres, a strong relationship between mean ground pressure and soil stress was observed, with a mean coefficient of determination of  $R^2 = 0.97$  (Schjønning et al., 2012). The current study indicates that the relationship may be true across types of undercarriage systems and tyres; excluding the dump truck's fourth axle from the

regression in Fig. 5A, results in  $R^2 = 0.95$ .

The increase in soil stress with increasing mean ground pressure was greater at 0.2 m than at 0.4 m depth, which would also be expected from classical stress propagation theory in soil (Boussinesq, 1885; Söhne, 1953), similar as reported for agricultural vehicles (e.g., Horn et al., 1998; Keller et al., 2016; O'Sullivan et al., 1999). Contrastingly, soil stress at 0.2 m and 0.4 m depth beneath access materials seemed little affected by mean ground pressure (Fig. 5A). This can be explained by a combination of two mechanisms. Firstly, the access material adds additional thickness which reduces stress as it propagates through an extra depth. Secondly, when two materials of different stiffness are in contact, the material with the higher stiffness concentrates the stress (de Lima and Keller, 2021; Keller et al., 2014). Consequently, the relative soil mean normal stress (i.e., the ratio of stress under access material to stress in unprotected soil) at both 0.2 and 0.4 m soil depth decreased with increasing mean ground pressure (Fig. 5B). This shows that the use of access material is particularly important at high mean ground pressures. Relative mean normal stresses per axle, soil depth, and access material are presented in **Supplementary Fig. S4**.

Differences in stress reduction between the three different access materials were small (Fig. 4, Fig. 5), despite differences in their characteristics (Table 1). Numerical simulations showed that this resulted from the combination of the access material thickness and Young's modulus, which caused comparable stress reductions for the tested access materials (Fig. 6a). Simulations revealed that stress reduction increases linearly with increasing access material thickness (Fig. 6b), and linearly with the natural logarithm of Young's modulus (Fig. 6c), which supports this study's third hypothesis. The simulations add valuable insights for managing soil stress reduction in practice, which may also be useful in other sectors than infrastructure construction such as forestry where the use of soil protection material is investigated (e.g., Solgi et al., 2018). For example, our simulations showed that achieving a stress reduction factor of 0.3 (equalling a relative stress of 0.7) at 0.4 m depth using a material with the stiffness comparable to a sand track as used in this study (Young's modulus of 3000 kPa) requires a thickness of 0.8 m, whilst the same stress reduction could be achieved by using a 0.1 m thick material with a Young's Modulus of 50 GPa (representing composites, metals, and (porous) ceramics).

### 3.3. Practical implications and conclusion

All the access materials tested in this study reduced soil stress at 0.2 and 0.4 m depth. Differences in soil mean normal stress beneath the three tested materials exhibited little variation, which was explained by the effect of the interaction of the material's thickness and Young's modulus on the stress reduction. The reduction increased with increasing mean ground pressure and was thus larger beneath tyres (47–77 %) than tracks (0–42 %).

As shown in this study, the properties (e.g., Young's modulus) and geometry (i.e., thickness) of access material impact soil stress reduction and hence have a great influence on soil protection. Further reduction of soil stress, hence reduction of the risk of soil compaction, can be achieved by increasing the thickness or stiffness of a material. In practice, the choice of access material will also depend on the accessibility, durability, the price of the material, transportation, and the ease of handling the material on-site, among other aspects.

Stiffer materials are generally more expensive but easier to transport and handle. For example, the price per running metre of the access materials used in this study were about CHF 20,- for the sand track, CHF 750,- for the timber mattresses (CHF 1'200 per mattress) and approximately CHF 1'500,- (CHF 3'500,- per plate), or CHF 15,- (CHF 25,- per plate) per week rental, for the composite mats (Hurni Kies und Beton AG, personal information, 07 March 2025). Yet as stiffer materials require less volume to establish an access road of a given length, the number of truck movements to bring the access material to the site were fewest for the composite mats, followed by the timber mattresses and the

sand track. Moreover, the ease of handling on-site was greatest for the composite mats and required least movements on the unprotected soil surface, followed by the timber mattresses and the sand track.

## CRediT authorship contribution statement

**Lorraine ten Damme:** Writing – review & editing, Writing – original draft, Visualization, Investigation, Formal analysis, Conceptualization. **Matthias Stettler:** Writing – review & editing, Resources, Investigation, Conceptualization. **Renato P. de Lima:** Writing – review & editing, Investigation. **Thomas Keller:** Writing – review & editing, Investigation, Funding acquisition, Conceptualization.

## Funding

This study was partly funded through the Conference of European Directors of Roads (CEDR) Transnational Road Research Programme, 2019 Call on Soils.

## Declaration of competing interest

The authors declare that they have no known competing financial interests or personal relationships that could have appeared to influence the work reported in this paper.

## Acknowledgements

The field work behind this research was largely organised by Hans Peter Kocher (Hurni Kies und Beton AG) in Switzerland, for which we are forever grateful. We thank the Bern University of Applied Sciences (HAFL) for providing the Bolling probes and Mario Stettler (HAFL) for managing the soil stress measurements, and Janosch Gerber (Beratungsbüro Matthias Stettler) and the drivers of the vehicles (Hurni Kies und Beton AG) for their assistance during the field measurements. Thanks too to Franziska Häfner, Olivier Heller and Lena Weiss from Agroscope for taking the soil samples and to Valerio Volpe and Marlies Sommer from Agroscope for guidance of laboratory measurements.

## Appendix A. Supplementary data

Supplementary data to this article can be found online at <https://doi.org/10.1016/j.jterra.2025.101097>.

## References

Anthony, M.A., Bender, S.F., van der Heijden, M.G.A., 2023. Enumerating soil biodiversity. *Proc. Natl. Acad. Sci.* 120. <https://doi.org/10.1073/pnas.2304663120>.

Ashok Kumar, A., Tewari, V.K., Gupta, C., Pareek, C.M., 2017. A device to measure wheel slip to improve the fuel efficiency of off road vehicles. *J. Terramechanics* 70, 1–11. <https://doi.org/10.1016/j.jterra.2016.11.002>.

Bates, D., Mächler, M., Bolker, B., Walker, S., 2015. Fitting Linear Mixed-Effects Models Using lme4. *J. Stat. Softw.* 67, 1–48. <https://doi.org/10.18637/jss.v067.i01>.

Berli, M., Eggers, C.G., Accorsi, M.L., Or, D., 2006. Theoretical Analysis of Fluid Inclusions for In Situ Soil Stress and Deformation Measurements. *Soil Sci. Soc. Am. J.* 70, 1441. <https://doi.org/10.2136/sssaj2005.0171>.

Berli, M., Kirby, J.M., Springman, S.M., Schulin, R., 2003. Modelling compaction of agricultural subsoils by tracked heavy construction machinery under various moisture conditions in Switzerland. *Soil Tillage Res.* 73, 57–66. [https://doi.org/10.1016/S0167-1987\(03\)00099-0](https://doi.org/10.1016/S0167-1987(03)00099-0).

Bolling, I., 1987. Bodenverdichtung und Triebkraftverhalten bei Reifen: Neue Mess- und Rechenmethoden. PhD Thesis. Tech. Univ. München, Ger.

Boussinesq, J., 1885. "Application des potentiels à l'étude de l'équilibre et des mouvements des solides élastiques" (Gauthier-Villars: Paris, France).

civiltoday, n.d. Bulk Density of Sand [WWW Document]. URL <https://civiltoday.com/civil-engineering-materials/sand/299-bulk-density-of-sand> (accessed 8.21.25).

de Lima, R.P., Keller, T., 2021. Soil stress measurement by load cell probes as influenced by probe design, probe position, and soil mechanical behaviour. *Soil Tillage Res.* 205, 104796. <https://doi.org/10.1016/j.still.2020.104796>.

Eggers, C.G., Berli, M., Accorsi, M.L., Or, D., 2006. Deformation and permeability of aggregated soft earth materials. *J. Geophys. Res. Solid Earth* 111, 1–10. <https://doi.org/10.1029/2005JB004123>.

European Commission: Joint Research Centre, AKCA, E., ALDRIAN, U., ALEWELL, C., ANZALONE, E., ARCIDIACONO, A., ARIAS NAVARRO, C., AUCLERC, A., AYDINSAKIR, K., BALLABIO, C., BALOG, K., BARAGAÑO, D., BARITZ, R., BELTRANDI, D., BERNATEK-JAKIEL, A., BØE, F., 2024. The state of soils in Europe. Publications Office of the European Union, Luxembourg.

FAO, ITPS, 2015. Status of the World's Soil Resources (SSWR) - Main Report. Food and Agriculture Organization of the United Nations and Intergovernmental Technical Panel on Soils, Intergovernmental Technical Panel on Soils. Rome, Italy.

Gartrell, C.A., Newman, J.K., Anderton, G.L., 2009. Performance Measurements of Pavement Matting Systems by Full-Scale Testing over Differing Soil Strengths. *J. Mater. Civ. Eng.* 21, 561–568. [https://doi.org/10.1061/\(ASCE\)0899-1561\(2009\)21:10\(561\)](https://doi.org/10.1061/(ASCE)0899-1561(2009)21:10(561)).

Horn, R., Mordhorst, A., Fleige, H., 2021. Consequences of gas pipeline hauling on changes in soil properties over 3 years. *Soil Tillage Res.* 211, 105002. <https://doi.org/10.1016/j.still.2021.105002>.

Horn, R., Richards, B.G., Gräslé, W., Baumgartl, T., Wiermann, C., 1998. Theoretical principles for modelling soil strength and wheeling effects - a review. *Zeitschrift für Pflanzenernährung und Bodenkd.* 161, 333–346.

Horn, R., Taubner, H., Wuttke, M., Baumgartl, T., 1994. Soil physical properties related to soil structure. *Soil Tillage Res.* 30, 187–216. [https://doi.org/10.1016/0167-1987\(94\)90005-1](https://doi.org/10.1016/0167-1987(94)90005-1).

Janzen, H.H., 2005. Soil carbon: A measure of ecosystem response in a changing world? *Can. J. Soil Sci.* 85, 467–480. <https://doi.org/10.4141/S04-081>.

Jenane, C., Bashford, L.L., Monroe, G., 1996. Reduction of Fuel Consumption Through Improved Tractive Performance. *J. Agric. Eng. Res.* 64, 131–138. <https://doi.org/10.1006/jaer.1996.0054>.

Keller, T., Berli, M., Ruiz, S., Lamandé, M., Arvidsson, J., Schjønning, P., Selvadurai, A.P. S., 2014. Transmission of vertical soil stress under agricultural tyres: Comparing measurements with simulations. *Soil Tillage Res.* 140, 106–117. <https://doi.org/10.1016/j.still.2014.03.001>.

Keller, T., Ruiz, S., Stettler, M., Berli, M., 2016. Determining Soil Stress beneath a Tire: Measurements and Simulations. *Soil Sci. Soc. Am. J.* 80, 541. <https://doi.org/10.2136/sssaj2015.07.0252>.

Lenth, R.V., 2024. emmeans: Estimated Marginal Means, aka Least-Squares Means. R Package. version 1 (10), 2.

Najafi, F., Thompson, K.A., Carlyle, C.N., Quideau, S.A., Bork, E.W., 2019. Access Matting Reduces Mixedgrass Prairie Soil and Vegetation Responses to Industrial Disturbance. *Environ. Manage.* 64, 497–508. <https://doi.org/10.1007/s00267-019-01193-4>.

Newpark Resources, Inc., n.d. DURA-BASE®, Advanced-composite mat system TM - The Path of Innovation is Paved with DURA-BASE. 1-877-MAT-ROAD 1–8.

O'Sullivan, M.F., Henshall, J.K., Dickson, J.W., 1999. A simplified method for estimating soil compaction. *Soil Tillage Res.* 49, 325–335.

R Core team, 2024. R: A Language and Environment for Statistical Computing. R Foundation for Statistical Computing, Vienna, Austria. <https://www.R-project.org/>.

Schjønning, P., Lamandé, M., Keller, T., Pedersen, J., Stettler, M., 2012. Rules of thumb for minimizing subsoil compaction. *Soil Use Manag.* 28, 378–393. <https://doi.org/10.1111/j.1475-2743.2012.00411.x>.

Söhne, W., 1953. Druckverteilung im Boden und Bodenverformung unter Schlepperreifen. (Pressure distribution in the soil and soil deformation under tractor tyres). *Grundlagen der Landtechnik* 49–63.

Solgi, A., Naghdi, R., Labelle, E.R., Zenner, E.K., 2018. The effects of using soil protective mats of varying compositions and amounts on the intensity of soil disturbances caused by machine traffic. *Int. J. For. Eng.* 29, 199–207. <https://doi.org/10.1080/14942119.2018.1527174>.

Stolte, J., Tesfai, M., Keizer, J., Øygarden, L., Kværnø, S., Verheijen, F., Panagos, P., Ballabio, C., Hessel, R., 2015. Soil threats in Europe: status, methods, drivers and effects on ecosystem services. JRC Scientific and Technical Reports. <https://doi.org/10.2788/828742>.

The European Parliament and the Council, 2015. Directive (Eu) 2015/719. Off. J. Eur. Union 115, 10.

Thompson, K.A., James, K.S., Carlyle, C.N., Quideau, S., Bork, E.W., 2022. Timing and duration of access mat use impacts their mitigation of compaction effects from industrial traffic. *J. Environ. Manage.* 303, 114263. <https://doi.org/10.1016/j.jenvman.2021.114263>.